

RESULTS OF THERMAL-SHOCK MODELING & ANALYSES FOR THE NATIONAL SPALLATION NEUTRON SOURCE

by

Rusi P. Taleyarkhan, Seokho H. Kim, John R. Haines
Oak Ridge National Laboratory
Oak Ridge, Tennessee, 37831, USA

ABSTRACT

An overview is provided on preliminary observations from simulations of thermal shock in the National Spallation Neutron Source (NSNS) at various power levels. The simulation framework being utilized and under development is presented. Results of simulations for pressure and stress profiles at key locations are presented. Variation of results with possible onset of mercury cavitation were modeled and the results are discussed. Significant reductions in stresses on structures may be possible with cavitation onset. Key thermal-shock related issues are highlighted.

INTRODUCTION

The National Spallation Neutron Source (NSNS) is a user facility providing high flux neutron beams for material research, isotope production, etc. The US Department of Energy has designated Oak Ridge National Laboratory (ORNL) to prepare a conceptual design for a next-generation, short-pulse spallation neutron source. This effort is working towards commencement of operation of the NSNS facility in 2004, with a cooperative effort between multi-national laboratories including ORNL, Lawrence Berkeley National Laboratory (LBNL), Los Alamos National Laboratory (LANL), Brookhaven National Laboratory (BNL) and Argonne National Laboratory (ANL). General information related to NSNS is provided elsewhere.¹ This paper concentrates primarily on operational safety-related work dealing with thermal-shock issues.

For spallation neutron sources, powers in the 1 MW range (time-average) are close to present technology limits resulting in the storing of around 1 to 2 x 10¹⁴ protons in each pulse. Also, designing targets for these high powers is very difficult. It is generally believed that, the

shock loads, radiation damage and heat dissipation requirements on a multi-MW-level target are thought to require designs beyond state-of-the-art.

The reference target design of the NSNS incorporates mercury as its reference target material. The mercury target design configuration, shown in Figure 1, has a width of 400 mm, a height of 100 mm, and a length of 650 mm. The mercury is contained within a structure made from 316-type stainless steel. Mercury enters from the back side (the side furthest from the proton beam window) of the target, flows through a 224 mm x 8 mm rectangular passage in the middle of the target to the front surface (proton beam window), and returns along the two side walls. The target window (i.e., portion of the target structure in the direct path of the proton beam) is cooled by mercury which flows through the passage formed between two walls of a duplex structure. In this way, the window cooling and transport of heat deposited in the bulk mercury are achieved with separate flow streams. This approach is judged to be more reliable and efficient (minimal pressure drop and pumping power) than using the bulk mercury to cool the window.

The duplex structure used for the window has significant structural advantages that help to sustain other loads. Beside serving as flow guides, the baffle plates used to separate the inlet and outlet flow streams are also important for maintaining the structural stability of the target. A safety container made from austenitic steel is provided around the mercury target to guide the mercury to a dump tank in the event of a failure of the target container structure.

The mercury target and its enclosing structure must be designed to sustain the time-averaged as well as peaked (during single pulse operation) power loads. These time-averaged and

single pulse loads for a 1-MW design are defined in Table 1. Since about 60% of the proton beam power is deposited in the mercury and balance into the surrounding structures, the thermal-hydraulic system for the target is designed to remove a time-averaged power of 0.6 - 1.2 MW corresponding to proton beam powers of 1 - 2 MW. For a pulse frequency of 60 Hz, the amount of energy deposited in the target during a single pulse is 10 - 20 kJ.

The interaction of the energetic proton beam with the mercury target leads to very high heating rates in the target. Although the resulting temperature rise is relatively small (a few °C), the rate of temperature rise is enormous ($\sim 10^7$ °C/s) during the very brief beam pulse (~ 0.58 μ s). The resulting compression of the mercury leads to the production of large amplitude pressure waves in the mercury that interact with the walls of the mercury target and the bulk flow field. Safety-related operational concerns exist in two main areas, viz., (1) possible target enclosure failure from impact of thermal shocks on the wall due to its direct heating from the proton beam and the loads transferred from the mercury compression waves, and (2) impact of the compression-cum-rarefaction wave-induced effects such as fluid surging and potential cavitation.

This paper describes ongoing modeling and analyses to establish the feasibility of using a liquid target (mercury) in the intense thermal load environment expected for the NSNS target system. A key ingredient in this study concerns the possible onset of cavitation in the mercury fluid at steel-mercury interfaces and in the bulk material itself. Results of initial studies to understand the implication of the onset of this effect are presented.

MODELING AND ANALYSIS FRAMEWORK

Understanding and predicting propagation of pressure pulses in the target (either liquid or solid) are considered to be critical for establishing the feasibility of constructing and safely operating such a device. The CTH code system² is being used as a basis for developing the appropriate simulation framework. CTH is a three-dimensional (3-D), shock-physics code, sometimes loosely referred to as a hydrocode. This code and associated technology base have been used extensively to simulate explosive processes (such as molten metal-water vapor explosions, and

hydrogen detonation) in enclosed fluid-structure systems.³⁻⁵ It is now being adopted for characterizing the current thermal-shock process in a coupled manner, simultaneously accounting for localized compression pulse generation due to rapid heat deposition, the transport of the compression wave through the mercury, interaction of this wave with the surrounding structure, feedback to the mercury from these structures, and multi-dimensional reflection patterns including rarefaction-induced material fracture (or possible cavitation phenomena in fluids).

Modeling and analysis work are being performed in several areas. Modeling is conducted in a staged manner starting with a simple two-dimensional (2-D) geometry, followed by full-scope 3-D model development.

Initial modeling efforts examined the effects of rapid heat deposition in an idealized axisymmetric target geometry with only an axially-varying transient heat deposition profile in mercury and steel in which 5 MW (60 Hz) of axially-varying energy deposition occurs, with each pulse lasting for 0.58 μ s. Results of this study have been reported previously⁶. These previously-reported studies had not included the aspect of radial and axially-variant energy deposition, and the possible impact of onset of cavitation.

Figure 2 provides a summary of axial and radial variations of the beam energy deposition profiles in mercury for a 1-MW NSNS. As seen, significant variations are to be expected in the instantaneous energy deposition in various locations of the target. In the radial direction (i.e., from beam centerline) the energy deposition drops almost exponentially with distance. In the axial direction, however, the beam peaks a few cm away from the front window and then drops off rapidly. In the study reported herein, two dimensional modeling was performed for a cross-section of the NSNS target (as shown in Figure 3). The cross-sectional variation of energy deposition was simulated at the axial position corresponding to a limiting location in the target.

The following key assumptions were made:

- 1) Mercury and steel interfaces will be characterized by perfect contact. This assumption was necessary to permit modeling to proceed,

although it is recognized that imperfect contact between mercury and steel is a possibility. The interface between mercury and steel is allowed to slide relative to each other as may be expected in the absence of alloying-type reactions at the interface.

2) The Mie-Grünesien (MG) equation-of-state (EOS) ⁷ adequately represents the mercury liquid at 100 C in compression and tensile states. The MG-EOS is well-known to be useful for use for materials in the compression state. It is recognized, however, that extension to tensile states may not be adequate especially when gaseous or vaporous cavitation may occur below a certain pressure threshold.

3) Cavitation onset (if modeled) will take place if the pressure in mercury goes below -1.0 MPa. It is well-known that fluids can sustain negative pressures prior to cavitation. The precise value of this threshold value depends on variables such as apparatus cleanliness, thermal states, loss of adhesion between fluid and structure, impurities in the fluid, etc. The value of -1.0 MPa for this initial study was based on the lower end of data taken by Briggs⁸ in thin-wall capillaries where the threshold for onset of cavitation was found to range from -0.7 MPa (for largely gaseous-type cavitation) to -40 MPa (for largely vaporous-type cavitation) depending on how the testing was conducted. Based on Briggs's data referenced herein it is recognized that, for NSNS operating conditions this value may be different from -1.0 MPa used in this current study. Experiments are planned to obtain NSNS-specific information.

4) While modeling cavitation the complex effects of any non-condensable gases generated via gaseous cavitation are negligible. This assumption "presumes" (for modeling convenience) that only vaporous-type cavitation will take place. The impact of dissolved gas evolution and system transport on thermal shock effects is an issue which is to be studied in the future.

5) Thermal energy transfer from mercury to the steel is negligible. This assumption is valid for the relatively short durations (~ 200 micro seconds) of time for thermal shock studies reported herein. It is recognized, however, that for longer durations approaching the time constant of the shell structures, thermal energy transfer will need to be accounted for.

Modeling of cavitation

As a simplified explanation, modeling of cavitation for this initial study was done via specification of a certain pressure level below which mercury is allowed to "fracture" and generate a cell void (i.e., "crack") which grows to absorb energy of the rarefaction (tensile) wave front (thereby maintaining the pressure reduction in the fluid to the threshold value). Upon arrival of a compression wave, the "fractured" mercury is allowed to heal and the process repeats itself until a sufficiently robust tensile wave front arises. Clearly, it is recognized that this solid-mechanics-based treatment does not model all thermal-shock phenomena associated with true cavitation (viz., dissolved gas evolution / transport and vapor bubble growth with subsequent collapse resulting in shock pressures - all in an intense ionizing medium, jetting, etc.). However, for scoping studies the gross aspects of void growth and collapse are simulated in the present model for estimating the relative impacts of the onset of cavitation versus the case where cavitation does not take place.

RESULTS OF SIMULATIONS

Simulations were conducted with and without invoking the fracture modeling features of CTH. In order to evaluate only the change in induced stresses into the steel walls, the system was initialized to remain at the mercury system pressure of ~0.3 MPa. Selected results of simulations with and without invoking onset of cavitation in the mercury are shown in Figures 4 through 5. The locations at which transient variations of pressure and stress values are indicated in Figure 3.

In the absence of cavitation, it is seen from Fig. 4a that negative (rarefaction wave) pressures in mercury imply that mercury can support a rarefaction process. This result is an artifact of assuming a solid-like equation-of-state (EOS) for mercury (Mie-Grünesien form)⁷ and the presumption that liquid mercury will not cavitate. It is realized that developing a more realistic EOS model for mercury in the regime expected in the NSNS target, along with simulation of more realistic physics of cavitation and geometry are required to improve our understanding and predictive capabilities. It is also seen from Figs. 4a

that, for the geometry under investigation, negative fluid pressures will vary from ~ -30 MPa at the central location (point 1) to ~ -10 MPa at the wall regions. Comparing these values with data taken in the past it is apparent that cavitation of mercury can not be ruled out, neither in the bulk region, nor at the mercury-steel interfaces.

Representative stress values (minimum principal stresses and maximum shear) at selected locations in the steel shell are shown in Fig. 4b. An interesting feature of stress variations is noted herein. Due to extreme variations in impedance between steel and air (at point 5) pressure waves at such locations undergo high-frequency ringing as waves bounce off at the gas-steel end of the steel structure. This is in sharp contrast to the steel baffle which has mercury on both sides of it (point 4) where such behavior is absent. The implications of such variations need to be taken into account from the viewpoint of fatigue cycle-induced failure introduced on to the steel structure at different locations.

Results of fluid pressure variations with cavitation onset at -1 MPa are displayed in Fig 5a at various locations (identified in Fig. 3). As can be seen, only compressive states are present and peak pressures are generally smaller than in the case which allows for cavitation (which is attributed to energy absorption in the fluid during fracture).

The variation of minimum principal stresses and maximum shear at selected locations are also shown in Fig. 5b. Clearly, as may be seen from Fig. 5b the level of induced stresses at critical locations such as the baffle (Point 4) are significantly ($> 50\%$) lower than if cavitation phenomena were not permitted to take place.

In a high irradiation field, it is known that the materials will show some embrittlement due to gas generation and atomic displacements. The failure mechanism may then progress due to crack propagation. However, data taken by M. Grossbeck at ORNL indicates little reduction ($< 20\%$) upon irradiation in cyclic stress limits for SS-316.⁹ The cyclic stress loads from the current study were found to be manageable when compared with allowable fatigue limits as suggested in the well-known ASME Boiler & Pressure Vessel Code although no data exists for high-cycle fatigue failure for SS-316 in a mercury

environment. Such data are in the process of being developed at ORNL.

SUMMARY AND CONCLUSION

To summarize, scoping assessments for thermal shock in the NSNS operating at the 1-MW power level have indicated the possibility of inducing significant tensile stresses in the fluid space. Coupled with the intense radiation environment these negative stress states in the fluid will likely result in onset of cavitation. It is too early to tell if such an occurrence has a net benefit (e.g., enhanced energy absorption) or a detriment (e.g., damage potential to the surrounding structures such as pitting, erosion, etc.). Several other areas related to impacts on the fluid field have been identified such as possible flow surging, enhanced mixing, etc.

A simulation framework has been developed along with a methodology to capture gross effects of cavitation onset and collapse. Results have been obtained with and without simulation of cavitation-like effects. These results indicate a substantial reduction of potentially-damaging fluctuating loads in the steel pressure boundary. Close to 50% reductions were noted in tensile loads as well as for maximum shear stress at selected locations. The complexities and associated uncertainties involved with such an assessment have been highlighted.

REFERENCES

1. T.A. Gabriel, et.al., "Overview of the NSNS Target Station," *Proc. of International Topical Meeting on Advanced Reactor Safety, ARS'97*, Orlando, Florida (1997).
2. J.M. McGlaun and S.L. Thompson, "CTH: A Three-Dimensional Shock-Wave Physics Code," *International Journal of Impact Engineering*, Vol.10, p.251-360 (1990).
3. V. Georgevich and R.P. Taleyarkhan, "Deterministic Method of Evaluating Multidimensional Explosive Loads Generated by Fuel Coolant Interaction in Uranium-Aluminum Fueled Reactors," *Transaction, Annual American Nuclear Society Conference*, November 14-19 (1993).
4. R.P. Taleyarkhan, et.al., "Analysis and Modeling of Flow-Blockage Induced Steam Explosion Events in the High Flux Isotope

- Reactor,” *Nuclear Safety Journal*, Jan.-June (1994).
5. R.P. Taleyarkhan, et.al., “Modeling and Analysis of Hydrogen Detonation Events in the Advanced Neutron Source Reactor Containment,” *Proc. Third International Conference on Containment Design and Operation*, Toronto, Canada (1994).
 6. R. P. Taleyarkhan, et al., “Thermal Shock Assessments for the NSNS Target System,” *Proc. of Intl. Topical Meeting on Advanced Reactor Safety (ARS’97)*, Orlando, Florida, June 1-5, 1997.
 7. H.A. Spetzler, M.D. Meyer and T. Chen, “Sound Velocity and Equation of State of Liquid Mercury and Bismuth at Simultaneous High Pressure and Temperature,” *Journal of High Temperatures - High Pressures*, **Vol. 7**, p.481-496 (1975).
 8. L. Briggs, “The Limiting Negative Pressure of Mercury in Pyrex Glass,” *Journal of Applied Physics*, Vol. 24, No. 4, April 1953.
 9. M. L. Grossbeck and K. C. Liu, “Fatigue Behavior at 650 C of 20% Cold-Worked Type 316 Stainless Steel Irradiated at 550 C in the High-Flux Isotope Reactor,” *ASTM Special Technical Testing Publication 870*, pp.732-744, (1985).
 10. P.L. Marston and B.T. Unger, “Rapid Cavitation Induced by the Reflection of Shock Waves,” *Shock Waves in Condensed Matter* (edited by Y.M. Gupta), p.401-405, *Proc. Fourth American Physical Society Topical Conference on Shock Waves in Condensed Matter*, Spokane, WA (1985).

Table 1. Power loads on the NSNS mercury target

| <u>Parameter</u> | <u>Value</u> |
|--|--------------|
| Energy of protons (GeV) | 1.2 |
| Pulse duration (μ s) | 0.5 |
| Pulse frequency (Hz) | 60 |
| Percent of beam power deposited in mercury target | 60 |
| <u>Time-Averaged Loads</u> | |
| Beam current (mA) | 1 - 2 |
| Total proton Beam Power (MW) | 1 - 2 |
| Peak beam power flux on target (MW/m^2) | 140-280 |
| Peak volumetric heating rate in mercury (MW/m^3) | 400 - 800 |
| Peak volumetric heating rate in window (MW/m^3) | 50 - 100 |
| <u>Loads During a Single Pulse</u> | |
| Energy per pulse (kJ) | 10 - 20 |
| Peak energy density in mercury (MJ/m^3) | 6.7 - 13 |
| Peak energy density in window (MJ/m^3) | 0.83 - 1.7 |

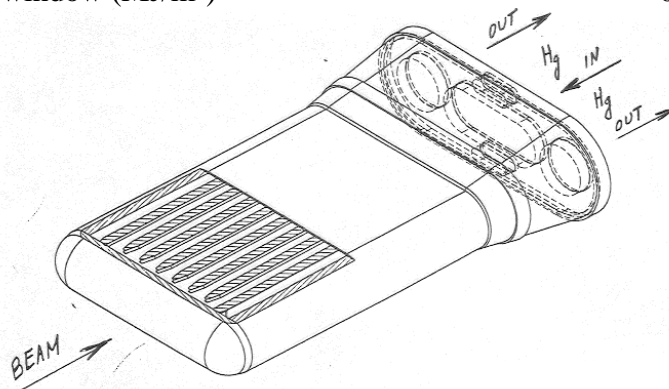


Figure 1. Schematics of NSNS Target System

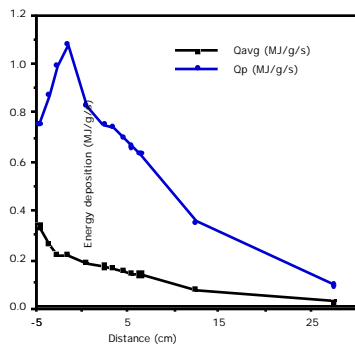


Figure 2a. Variation of peak and averaged energy deposition along length of proton beam in NSNS target

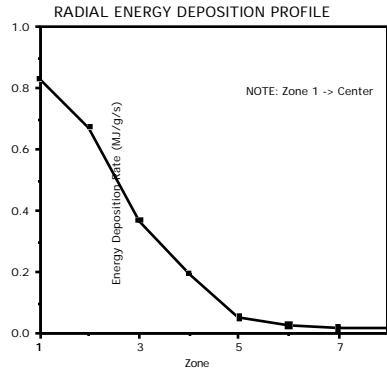
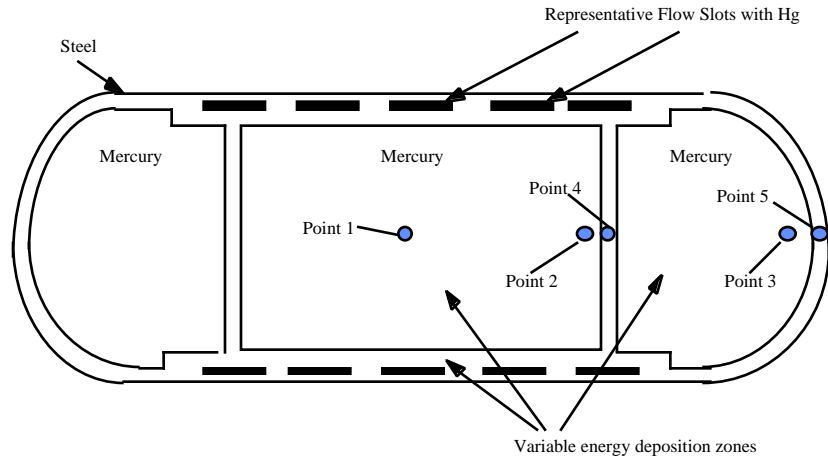


Figure 2b. Variation of energy deposition from central zone to outermost zone in NSNS mercury target



Notes (for 1-MW NSNS with 0.58 mic.sec. pulse):

- 1) Radial energy variation (= 0.83 MJ/g/s at center to 0.01 MJ/g/s at edges)
- 2) Mie-Gruniesen Equation-of-State (no cavitation)
- 3) Perfect contact of mercury with steel
- 4) Points 1, 2,3,4, and 5 are locations where pressure and stress variations are displayed in Figs. 4 & 5.

Figure 3. CTH Model Schematic of NSNS Target Cross-section